Agricultural Water Management 103 (2012) 182–190

Contents lists available at SciVerse ScienceDirect

Agricultural Water Management

journal homepage: www.elsevier.com/locate/agwat

Letter to the Editor

Influence of geometric design of alternate partial root-zone subsurface drip irrigation (APRSDI) with brackish water on soil moisture and salinity distribution

ARTICLE INFO

Keywords:
Alternate partial root-zone subsurface drip irrigation
Emitter depth
Inter-plant emitter distances
Soil salinity
HYDRUS-2D/3D
Egypt

ABSTRACT

In alternate partial root-zone irrigation (APRI) a significant amount of irrigation water can be saved without considerable yield reduction. In this paper, HYDRUS-2D/3D was used to investigate the impact of geometric design of alternate partial root-zone subsurface drip irrigation (APRSDI) with brackish water for growing tomato on soil moisture and salinity distribution. Three inter-plant emitter distances (IPED; 20, 30, and 40 cm), two emitter depths (10 and 20 cm), and three irrigation water salinity levels (0, 1, and 2 dS m^{-1}) were used to implement the proposed simulation scenarios in loamy sand soil during a 40-day simulation period. The simulation results showed that higher soil moisture content was found beneath the plant trunk in case of 20 cm (short IPED) and near the domain border in case of 30 and 40 cm IPED. Short IPED guarantees more water in the maximum root density zone. A deeper wetting front occurred for deep emitter depth, while the wetting front reached the soil surface for shallow emitter depth. Salinity results revealed that as irrigation water salinity increased, the salinity in the top soil increased. In addition, the salinity at the soil surface increased as IPED and emitter depth increased. Higher root water uptake rates were recorded in the case of 20 cm IPED while the emitter depth did not show any considerable effect on root water uptake rates. Moreover, the applied irrigation water was fully consumed by the plant in case of short IPED. Emitter depth and salinity of irrigation water had negligible effect on amount of irrigation water extracted by plant roots and percolated amount below the bottom boundary of the flow domain. Overall, short IPED is recommended in APRSDI with or without brackish irrigation water regardless of the emitter depth.

1. Introduction

Egypt is water scarce and considered to be over populated relative to its cultivated area (31.5 billion m^2; Hafez, 2005). About 85% of Egypt's water resources are used in agriculture that mainly depends on River Nile (55.5 billion m^3/year). Therefore, effective and wise use of Nile water in irrigation practices is an important way to cope with water scarcity and to make reclamation of new agricultural land possible. In this regard, modern irrigation techniques accompanied with using alternate water sources (e.g., agricultural drainage water) are considered a proper way to reduce the overuse of Nile water for irrigation purposes. The El-Salam Canal, a mixture of 2.1 billion m^3/year of fresh water from the River Nile and 1.9 billion m^3/year of drainage water, is used to irrigate 2.6 billion m^2 of new reclaimed areas in the Eastern Delta and North Sinai. Lately, modern irrigation techniques have caught Egyptian decision makers' attention as a promising and viable option to save water. Alternate partial root-zone irrigation (APRI) is such a technique in which a significant amount of irrigation water can be saved without considerable yield reduction (e.g., Du et al., 2005). In this technique, a part of the root system is exposed to drying soil while the remaining part is irrigated normally (e.g., Kang and Zhang, 2004). Shifting of irrigation between the two root halves depends on many factors such as the moisture content level in the drying soil, crop type, growing stage, soil texture, environmental conditions, and method of irrigation (e.g., Saeed et al., 2008). Due to these factors, no definite procedure exists for determining the optimum timing of irrigation of each side (Sepaskhah and Ahmadi, 2010).

The philosophy of APRI is founded on two theoretical concepts. The first concept is that luxury transpiration (water loss) occurs during full irrigation event due to wide stomatal opening. Thus, a small closure of the stomatal opening may minimize water loss without significant effect on photosynthesis (Stoll et al., 2000). The second concept is the ability of the root in drying soil to respond to the drying conditions by sending a root-sourced chemical signal from plant roots to leaves causing partial closure of stomata (Kang and Zhang, 2004). Sepaskhah and Ahmadi (2010) described the plant response mechanism during APRI as the root in irrigated side extracting enough water to keep high shoot water potential while the roots in the non-irrigated side producing more xylem abscisic acid (ABA), a plant hormone, to reduce the stomatal conductance and leaf area.

Water use efficiency and crop yield productivity for diverse plant species and soil types under APRI have been extensively investigated during the last decade. Shani-Dashtgol et al. (2006) compared ordinary and alternate furrow irrigation for growing sugar cane in a warm arid area. They concluded that 26% of the irrigation water was saved in alternate furrow irrigation with a 10% increase in crop production compared to ordinary furrow

0378-3774/$ – see front matter © 2011 Elsevier B.V. All rights reserved.
doi:10.1016/j.agwat.2011.11.013

irrigation. Du et al. (2006) compared three furrow irrigation treatments (conventional, fixed partial root-zone, and alternate partial root-zone furrow irrigation) for growing cotton using three irrigation levels. They concluded that alternate partial root-zone furrow irrigation resulted in highest yield for all irrigation level scenarios with higher water use efficiency. Processing tomato under APRI was investigated by Kidra et al. (2004) and their results showed that APRI reduced 50% of irrigation amount with a marginal yield reduction. Gencoglan et al. (2006) studied the effect of green bean yield under conventional subsurface drip irrigation (SDI) and APRSDI. They showed that APRSDI saved a significant amount of irrigation water (about 50%) with the same yield as for SDI. Similar finding was presented by Huang et al. (2010) when investigating potato yield using SDI and APRSDI. The effect of APRI on soil microorganism during growing maize was studied by Wang et al. (2008). They showed that the peak number of soil microorganism was obtained in APRI compared to conventional irrigation and fixed partial root root-zone irrigation.

Understanding water and salinity distribution under APRI for a wide range of soil types, crops, design features, and irrigation strategies by mean of field experiments are costly and time-consuming. The investigation of successive wetting and salinity patterns and root water uptake under APRI needs a detailed soil water monitoring and large number of measurements. Numerical modeling is, on the other hand, an inexpensive, rapid, and labor saving tool for simulating water and solute dynamics under different irrigation techniques. Numerical simulation studies of diverse irrigation methods (e.g., Phogat et al., 2010; Simunek and Hopmans, 2009; Hanson et al., 2008; Ajdary et al., 2007; Lazarovitch et al., 2005; Gardenas et al., 2005; Skaggs et al., 2004) revealed that HYDRUS-2D (Simunek et al., 2008) precisely simulates water and solute movement under different irrigation methods and soil types. Therefore, HYDRUS-2D can be used as an effective design and management tool.

Although a great number of numerical simulations have been conducted for water dynamics and solute transport under different irrigation methods during the last decade, few numerical simulation studies focused on soil moisture distribution under APRI (e.g., Zhou et al., 2007, 2008). Simulation of soil salinity distribution under APRI with brackish irrigation water has not yet been addressed by researchers. The majority of conducted research on APRI focused mainly on the physiological and morphological aspects of APRI on plants and its influence on yield and water productivity while there is a lack in research dealing with geometric design features. Therefore, it is essential to find effects and optimal geometric design when using brackish irrigation water on water flow and solute transport as well as water balance components under APRSDI. The present work was conducted to investigate the effect of IPED, emitter depth, and irrigation water salinity on soil moisture and salinity distribution as well as water balance components for the APRSDI system. We believe that this study will provide better guidelines for suitable irrigation management under APRSDI and it is very important to make these guidelines available to farmers and irrigation specialists.

2. Methods and materials

A numerical model for water flow and solute transport, HYDRUS-2D/3D (Simunek et al., 2008), was used to study the effect of IPED, emitter depth, and irrigation water salinity on soil water movement, salinity distribution, and water balance components under APRSDI system. HYDRUS-2D/3D can simulate water, heat, and solute movement in two- and three-dimensional variably saturated media under a wide range of complex and irregular boundary conditions and soil heterogeneities. The software uses a modified

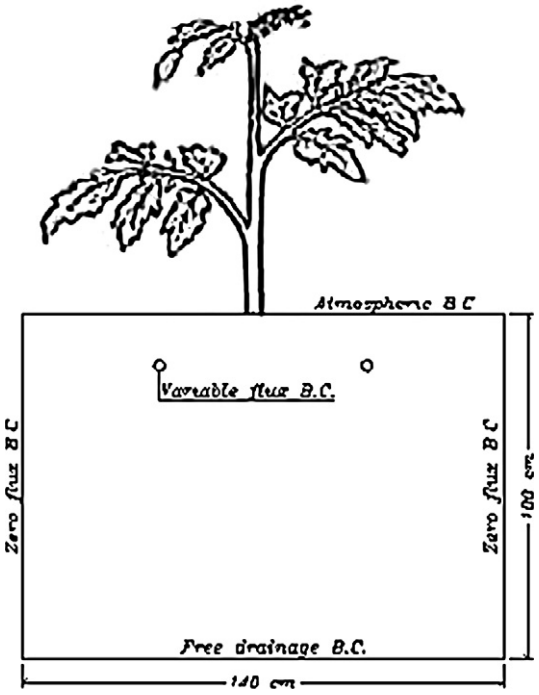

Fig. 1. Conceptual diagram of simulated area.

form of Richards' equation including a sink term for water uptake by plant roots to describe water flow in isotropic variably saturated porous media. Based on the mass conservative iterative scheme introduced by Celia et al. (1990), Galerkin finite element method is used to solve Richards' equation. Richards' equation (Richards, 1931) assumes that the air phase has no pronounced effect in liquid flow process and water flow owing to thermal gradients can be ignored. Numerical solutions of Richards' equation for water flow require knowledge of soil water characteristics (θ_s, saturated water content; θ_r, residual water content; α, related to the inverse of a characteristic pore radius; l, shape parameter; n, pore-size distribution index; $m = 1 - (1/n)$) and saturated hydraulic conductivity (K_s). On the other hand, molecular diffusion (D_m), transverse dispersivity (D_T), longitudinal dispersivity (D_L), and the adsorption isotherm constant (k_d) govern the solute transport process. HYDRUS-2D/3D uses the advection-dispersion equation (e.g., Hillel, 1998) to describe the solute transport considering advection-dispersion in the liquid phase as well as diffusion in the gaseous phase.

The simulated APRSDI system was assigned to irrigate tomato, a typical crop in El-Salam Canal cultivated land. Each tomato row had two subsurface drip lines, one on each side of tomato row. The distance between the tomato row and subsurface drip line was 20, 30, and 40 cm. The spacing between online emitters was 35 cm and the spacing between two tomato rows was 140 cm. The El-Salam Canal cultivated land is characterized by high annual potential evapotranspiration and low annual rainfall, approximately 150 mm/year. Maximum temperatures range from 41 to 46 °C during July and August while minimum temperatures vary from 8 to 19 °C during December and January (Rashed et al., 2003).

The simulated region was 100 cm deep and 140 cm wide for all simulation scenarios with a trickle emitter of radius 1 cm placed in the location of the drip line (Fig. 1). The drip line was simulated as an infinite line source (e.g., Skaggs et al., 2004). Unstructured triangular mesh was used to spatially discretize the flow domain with smaller size triangles near the surface and larger size triangles toward the bottom boundary. Mesh refinement was done at emitter

perimeter and closer to the soil surface where quick change in flux occurs.

A free drainage boundary condition was selected at the base of the flow domain. This boundary condition assumes a unit gradient along the lower boundary because the water table lies below the domain of interest (about 1.50 m below the soil surface). Zero flux boundary condition was set through the vertical edges of the flow domain due to symmetry. Top boundary was characterized by atmospheric boundary condition permitting crop evapotranspiration (ET_c). Based on the weather conditions, Penman–Monteith equation was used to calculate crop ET_c as a product of reference crop (ET_0) and crop coefficient value (K_c). K_c for tomato was 1.05 (Allen et al., 1998). During simulation, it was assumed that the crop had full canopy coverage. Therefore, potential transpiration was taken equal to potential evapotranspiration while the potential evaporation was neglected. The ET_c was assumed constant, $ET_c = 0.75\ cm\ d^{-1}$, during the entire simulation period. It is pertinent to note that the applied irrigation water was assumed 25% less than full irrigation when using conventional subsurface drip irrigation system. The irrigation flux was simulated using variable flux boundary condition along the emitter perimeter during irrigation (operating) time and no flux in the off time. The water flux (q) during the irrigation time was calculated based on emitter discharge of 1.0 l/h as

$$q = \frac{\text{Emitter discharge flow rate}}{\text{Drip tubing surface area}} = \frac{Q}{2\pi rS} = \frac{24,000}{2 \times \pi \times 1 \times 35} = 109.14\ cm\ d^{-1} \quad (1)$$

where Q is the emitter discharge ($L^3\ T^{-1}$), r is the emitter radius (L), and S is the distance between emitters (L). The irrigation period was 2.75 h per day and was estimated by dividing the applied irrigation water by the emitter discharge as

$$\text{Irrigation period} = \frac{0.75ET_c \times \text{soil surface area}}{\text{Emitter discharge}} = \frac{0.75ET_c \times w \times S}{Q} = \frac{0.75 \times 0.75 \times 140 \times 35}{24,000} = 0.115d \quad (2)$$

where w is the width of the soil surface associated with the transpiration process (L). The irrigation interval for each emitter was assumed two days where the two emitters were operated alternatively. Sepaskhah and Ahmadi (2010) stated that no definite procedure exists on determining the optimum timing of irrigation of each side. A third type Cauchy boundary condition along the emitter circumference was used to describe the effect of irrigation water salinity during a given irrigation events. In the present study, the solute was accompanied with the irrigation water and irrigation water salinity was taken equal to 0, 1.0, and 2.0 dS m^{-1} (the salinity of El-Salam Canal water ranges from 1.0 to 2.0 dS m^{-1}).

Initial water content and initial solute concentration within the flow domain were 0.199 $m^3\ m^{-3}$ and 2.0 dS m^{-1}, respectively. Abou Lila et al. (2005) showed that the soil salinity in El-Salam Canal cultivated land ranges from 0.70 to 3.50 dS m^{-1}.

Although, direct measurement of soil hydraulic parameters (θ_s, θ_r, α, l, n, and m) required for model execution in the laboratory is time-consuming and costly, these parameters were estimated using standard laboratory methods using a pressure plate apparatus for loamy sand soil samples collected from El-Salam Canal cultivated land. It is worth mentioning that the accuracy of simulation depends mainly on the quality of these parameters. Table 1 shows soil hydraulic parameters used for model execution. Solute parameters required for model execution were longitudinal dispersivity (ε_L) and transversal dispersivity (ε_T). The ε_L was taken equal to 10 cm that is equal to one-tenth of the profile depth (see e.g., Beven et al., 1993; Cote et al., 2001) while ε_T was set equal to $0.1\varepsilon_L$. Molecular diffusion and adsorption isotherms were ignored during simulation.

Table 1
Hydraulic parameters for simulated soil.

Soil type	θ_r	θ_s	α	n	k_s (cm d^{-1})	l
Loamy sand	0.074	0.453	0.045	1.72	288.5	0.5

Root water uptake affects the spatial distribution of soil salinity and soil water content between successive irrigation events. The Feddes model (Feddes et al., 1978) was used to simulate water uptake from the soil during simulation. The Feddes model calculates plant root water uptake rates according to the soil water pressure head at any point in the root zone. Table 2 shows the different pressure heads used in simulation that governed the root water uptake rates in the soil profile. The critical water stress index (w_c) value was set equal to 1 as in many other studies (e.g., Phogat et al., 2010; Hanson et al., 2008; Ajdary et al., 2007; Gardenas et al., 2005) and by Zhou et al. (2007) when simulating the APRI using the HYDRUS model. It is worth mentioning that agricultural plants have a relatively high w_c, therefore, their ability to compensate natural stresses is limited (Simunek and Hopmans, 2009).

The osmotic effect on the root water uptake rate was considered during simulation using the threshold model (Maas, 1990) with a slope of 9.90% and threshold EC_e of 2.5 dS m^{-1}. Due to lacking information on root distribution under the given simulation scenarios, root distribution for tomato crop was assumed constant with time and set according to Hanson et al. (2006; Fig. 2).

Simulations were carried out for a 40-day time period (summer season) considering three IPED (20, 30, and 40 cm), two emitter depths (10 and 20 cm), and three salinity levels for the irrigation water (0, 1, and 2 dS m^{-1}). Table 3 shows the different simulation scenarios used in the present study. To depict the temporal variation of soil moisture and salinity distribution during the entire simulation period, observation points were selected at certain locations within the flow domain.

3. Results and discussion

3.1. Soil moisture content patterns

For all simulation scenarios, although the initial moisture content was uniform throughout the flow domain, soil moisture

Table 2
Root water uptake parameters (after Feddes et al., 1978).

P0 (cm)	POpt (cm)	P2H (cm)	P2L (cm)	P3 (cm)
−1	−2	−800	−1500	−8000

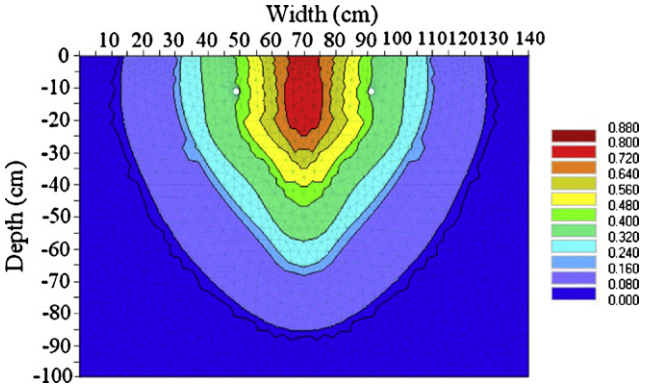

Fig. 2. Root distribution used for HYDRUS-2D simulation (units: percentages of the total roots; Hanson et al., 2006).

Table 3
Simulation scenarios.

Scenario number	Inter-plant emitter distance (cm)	Emitter depth (cm)	Salinity of irrigation water (dS m^{-1})	Scenario number	Inter-plant emitter distance (cm)	Emitter depth (cm)	Salinity of irrigation water (dS m^{-1})
1	20	10	0	10	20	20	0
2	20	10	1	11	20	20	1
3	20	10	2	12	20	20	2
4	30	10	0	13	30	20	0
5	30	10	1	14	30	20	1
6	30	10	2	15	30	20	2
7	40	10	0	16	40	20	0
8	40	10	1	17	40	20	1
9	40	10	2	18	40	20	2

content values differed with time and from point to point during simulation period. This variation depended mainly on irrigation occasion, root distribution in the flow region, soil hydraulic properties, IPED, and emitter depth. In general, at the commencement of each irrigation event, the soil moisture content was maximum adjacent to the emitter, then the wetting bulb increased in size in both directions (vertical and lateral). After ceasing irrigation, considerable reduction in water content occurred around the emitter due to redistribution and plant root extraction. Similar wetting and drying patterns took place reflecting the watering and subsequent root water uptake.

3.1.1. *Effect of inter-plant emitter distance on water content distribution*

The contour plots in Fig. 3 shows the spatial distribution of soil moisture content after the first irrigation event and at the termination of simulation period for simulation scenarios 1, 4, and 7. The size and shape of the wetting zone in all scenarios after the first irrigation event were almost identical. The vertical component of the wetted zone was larger than the horizontal with less water above the emitter than beneath. The wetted depth below the emitter was 22 cm while the horizontal water movement was limited to 17 cm at the depth of the emitter and water content reached the soil surface. Limited lateral extension of wetting bulb in all simulation scenarios strengthens the hypothesis that approximately half of plant root system was always exposed to drying cycle during simulation. During simulation, the maximum soil moisture content was 0.38 m^3 m^{-3} located near the emitter. It is worth mentioning that saturation near the emitter never occurred due to the low water holding capacity of the loamy sand which caused water to move rapidly away from the emitter by gravity. Simulation results also showed that at the end of the simulation period, a higher moisture content was observed near the domain boarders in case of long IPED (30 and 40 cm). This confirms that a significant amount of irrigation water was unavailable (untapped) for plant roots in the case of long IPED. The limited spreading of the wetting bulb obstructs movement of water toward the zone of maximum root density especially below the plant trunk. On the other hand, soil moisture content values in the region below the plant trunk were higher in case of 20 cm IPED compared to long IPED, especially for the top soil layer (0–20 cm). Therefore, short IPED is preferable to sustain a considerable amount of soil moisture in the zone of maximum root density.

3.1.2. *Effect of emitter depth on water content distribution*

The depth of wetting bulb depended mainly on emitter depth and soil hydraulic properties. As expected, when emitter depth increased, the depth of the wetting zone increased. The emitter depth also affected the upper limit of the wetting zone along the soil surface while the lateral extension of the wetting zone was unaffected. After the first irrigation event, the wetting front reached the soil surface for shallow emitter depth (10 cm) but not for the deep

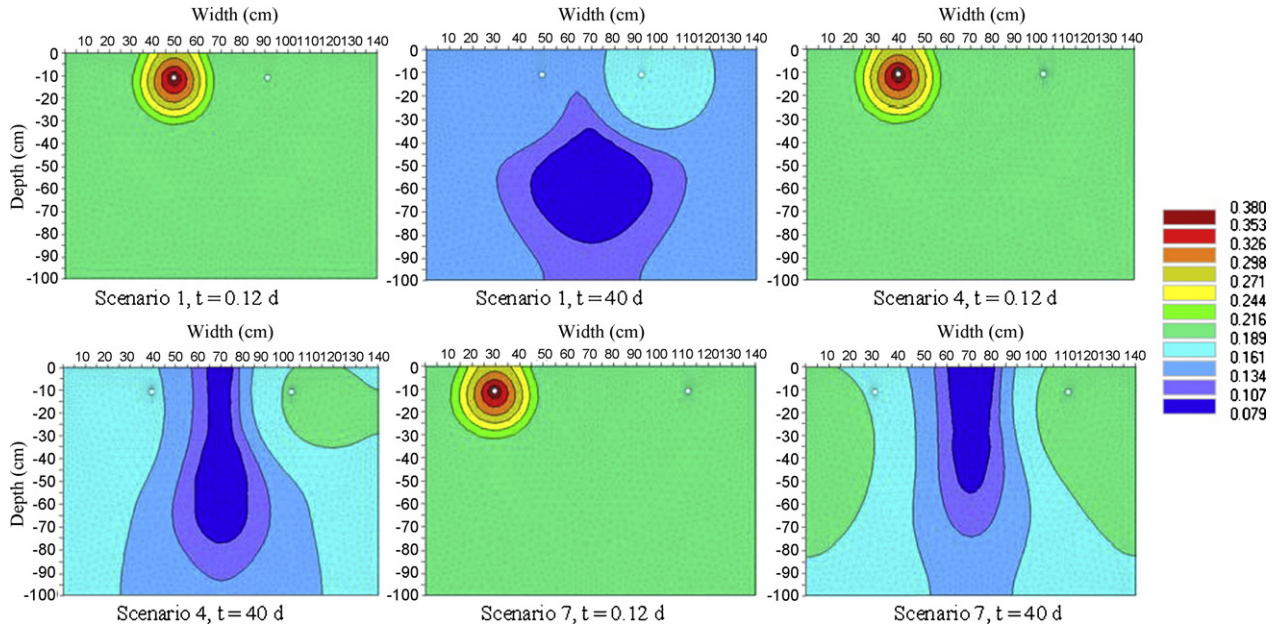

Fig. 3. Spatial distribution of soil moisture content after the first and last irrigation event for scenarios 1, 4, and 7 (IPED and emitter depth for scenarios 1, 4, and 7 are [20, 10]; [30, 10]; [40, 10], respectively; unit: m^3 m^{-3}; white dot indicates emitter location).

emitter depth (20 cm). The vertical extension above the emitter was only 16 cm in case of 20 cm emitter depth (data not shown). Fig. 4 shows the temporal variation in soil moisture content for both emitter depths at two observation points: one at the soil surface 10 cm away from the plant trunk (obs. 1) and the other located 20 cm directly below the plant trunk (obs. 2). A higher moisture content (0.25 $m^3\ m^{-3}$) was observed at the soil surface for shallow emitter depth and the fluctuations in moisture content were more distinct. These fluctuations were a combined result of successive soil water recharge during the irrigation events and water depletion by the plant roots and evaporation in the period between irrigation events. The fluctuations in soil moisture content were less pronounced in the case of deep emitter depth owing to that water did not reach soil surface at end of irrigation event. On the other hand, the emitter depth did not appear to have significant effect on the soil content at 20 cm depth below the plant trunk. Soil moisture content was approximately the same for both emitter depths during the entire simulation period.

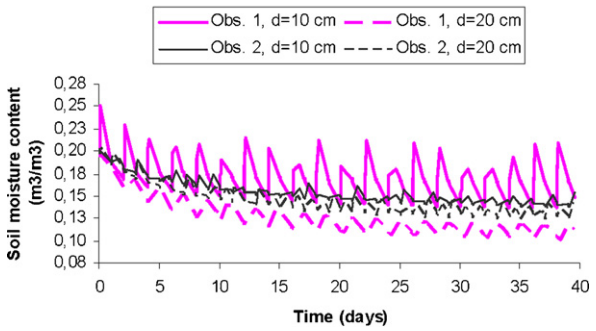

Fig. 4. Temporal variation in soil moisture content for scenarios 1 and 10 (IPED and emitter depth are [20, 10]; [20, 20], respectively). Obs. 1: at the soil surface 10 cm away from the plant trunk and obs. 2: at 20 cm directly below the plant trunk.

3.2. Root water uptake

Although the root distributions were the same for all simulation scenarios, the spatial distribution of root water uptake was different between scenarios. This is attributed to the variable distribution of soil moisture and salt concentration in the soil profile during the entire simulation period.

3.2.1. Effect of inter-plant emitter distance on root water uptake

Fig. 5 depicts the temporal variation in root water uptake for simulation scenarios 1, 4, and 7. For 20 cm IPED the root water uptake rate gradually decreased from 0.75 to 0.6 cm d^{-1} and decreased from 0.75 to 0.56 cm d^{-1} in case of 30 cm IPED. On the other hand, for 40 cm IPED, the root water uptake rate decreased dramatically from 0.75 to 0.57 cm d^{-1} during the first 10 days then it decreased gradually to 0.51 cm d^{-1} by the end of simulation period. The rapid reduction in root water uptake rates during the first 10 days was attributed to the limited extension of the wetting bulb. Nevertheless, the amount of water stored in the soil was not sufficient to compensate for the lack of irrigation water in the zone of maximum root density to keep the root water uptake rate at its higher levels. The IPED had a great impact on root water uptake rates. Therefore, short IPED is recommended in APRSDI especially for plants with limited root extension.

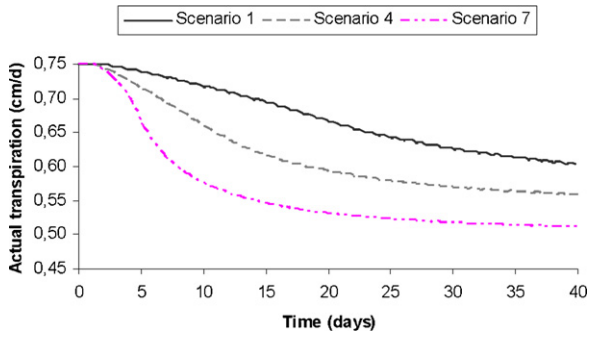

Fig. 5. Temporal variation in root water uptake under different IPED (20, 30, and 40 cm for scenarios 1, 4, and 7, respectively).

To test the sensitivity of the root water uptake rate to changes in the critical water stress index value (compensate root water uptake), additional simulations were conducted to model the compensation of water uptake using w_c values of 0.90 and 0.85. The results showed a limited increase in root water uptake compared to the compensation ratio as well as compared to the non-compensating root water uptake case.

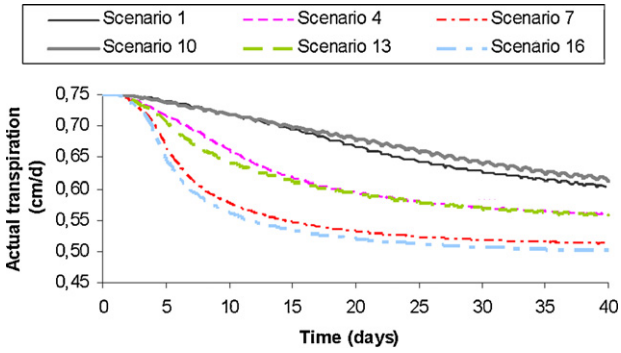

Fig. 6. Temporal variation in root water uptake under different IPED and emitter depths (IPED and emitter depth for scenarios 1, 4, 7, 10, 13, and 16 are [20, 10]; [30, 10]; [40, 10]; [20, 20]; [30, 20]; and [40, 20], respectively).

3.2.2. Effect of emitter depth on root water uptake

Fig. 6 presents the temporal variation in root water uptake for both emitter depths (10 and 20 cm). The root water uptake rate was approximately the same for both emitter depths at different IPED. The root water uptake rate was slightly higher (by 0.015 cm d^{-1}) for shallow emitter depth for all IPED with the only exception of 20 cm IPED. Therefore, the emitter depth had negligible effect on root water uptake rate in APRSDI. This contradicts findings of Selim et al. (2011, manuscript). They concluded that considerable higher root water uptake rates occur in case of shallow emitter depth under SDI for growing tomato in the same study area. Further studies are needed to clarify this discrepancy.

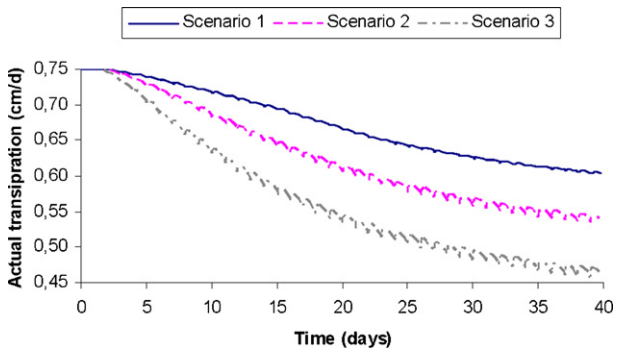

Fig. 7. Temporal variation in root water uptake under different irrigation water salinity levels (0, 1, and 2 dS m^{-1} for scenarios 1, 2, and 3, respectively).

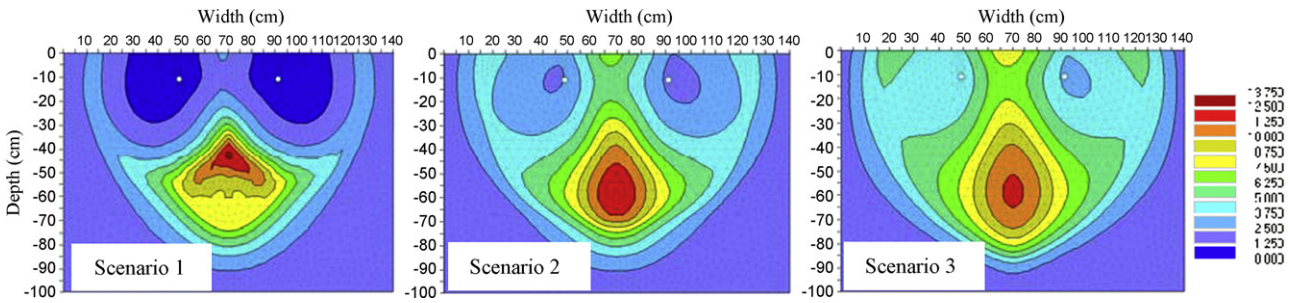

Fig. 8. Spatial distribution of soil salinity at the end of simulation period for different irrigation water salinity scenarios (irrigation water salinity = 0, 1, and 2 dS m^{-1} for scenarios 1, 2, and 3, respectively; unit: dS m^{-1}; and white dot indicates to the emitter location).

3.2.3. Effect of irrigation water salinity on root water uptake

Soil water and soil salinity levels in the root zone had great impact on root water uptake rate. Fig. 7 shows the temporal variation in root water uptake rate under different irrigation water salinities. As the irrigation salinity increased, the rate of water extracted by plant roots decreased due to salt stress effects. The root water uptake rate for non-saline irrigation water decreased from 0.75 to 0.6 cm d^{-1} by the end of the simulation period while it reached 0.54 and 0.46 cm d^{-1} for irrigation salinities of 1 and 2 dS m^{-1}, respectively. The effect of irrigation water salinity was more pronounced for long IPED. The root water uptake rate at the end of the simulation period for 40 cm IPED was 0.51, 0.46, and 0.39 cm d^{-1} for irrigation water salinities of 0, 1, and 2 dS m^{-1}, respectively. Therefore, long IPED is inappropriate when using brackish irrigation water.

3.3. Soil salinity distribution

Salt concentrations in the root zone and crop salinity tolerance are the major factors affecting the selection of cultivated crop and irrigation system. Transpiration and growth rates for a certain crop are largely influenced by the excess salinity in the root zone. For all simulation scenarios at the cease of the first irrigation event, reduction in soil salinity occurred near the emitter and an augment in salinity concentration occurred away from the emitter in both vertical and lateral directions.

3.3.1. Effect of irrigation water salinity on soil salinity distribution

Fig. 8 shows the spatial distribution of soil salinity by the end of simulation period for different irrigation water salinity scenarios. It was noted that for non-saline irrigation water, the leached soil volume increased as time evolved. At the end of the simulation period, considerable leaching occurred for the top 30 cm soil layer. Soil salinity was lower than the initial soil salinity level and higher salinity was observed between the 40 and 65 cm depths due to downward displacement of salt. For 1 and 2 dS m^{-1} irrigation water salinity scenarios, the amount of salt accumulated near the soil surface increased as time evolved. Higher salinity levels at the soil surface were noted at the location of the plant trunk, moreover, the maximum soil salinity levels were noted between the 50 and 70 cm depths. Higher salinity at soil surface negatively affects the seed germination and crop establishment. Therefore, APRSDI is more suitable with non-saline irrigation water especially in case of shallow root plants.

3.3.2. Effect of inter-plant emitter distance and emitter depth on soil salinity distribution

Fig. 9 shows the salinity distribution along a vertical section coinciding with the symmetry plane of flow domain for simulation scenarios 1, 4, and 7. Great variation in salinity levels was noted for the top 40 cm soil layer while the variation was less pronounced for deeper soil layers. Soil salinity at the top layers was higher in case of long IPED. Soil salinity at the top soil layer increased as IPED increased. Therefore, short IPED is recommended especially for shallow rooted plants.

The effect of emitter depth on soil salinity distribution is shown in Fig. 10. The figure shows the spatial distribution of soil salinity at the end of simulation period for scenarios 1 and 10. Soil salinity levels were the same in deep soil layers, however, it reached higher values at the soil surface in the case of deep emitter depth. This is attributed to the limited vertical extension of the wetting front above the emitter. The wetting front did not reach soil surface in the case of deep emitter depth while it extended for about 30 cm at soil surface in case of shallow emitter depth.

3.4. Water balance

Water balance components for all simulation scenarios are shown in Table 4. The data listed in Table 4 is expressed in percent of total applied water during the entire period of simulation (40 days). The applied irrigation water was fully consumed by plants in case of 20 cm and 30 cm IPED scenarios with the exception of 30 cm IPED with irrigation water salinity of 2 dS m^{-1}. The percent of applied water extracted by plant roots was relatively large for the 20 IPED scenarios and varied from 100 to 119% while it ranged from 94 to 110% for the 30 cm IPED scenarios. Thus, the joint effect of irrigation water salinity and emitter depth on the amount of applied water extracted by plant roots was negligible in case of 20 cm IPED (all applied water was effectively used by the plant). However, irrigation water salinity had a considerable effect in case of the 30 cm IPED. As the irrigation water salinity increased, the amount of water extracted by plant roots decreased. It should be noted that due to the deficit in irrigation water and the higher initial moisture content the plant consumed a significant amount of water stored in the root zone. The deficit in applied irrigation water was thus replaced by water stored in the root zone. On the other hand, the plant consumed about 86–99% of applied water

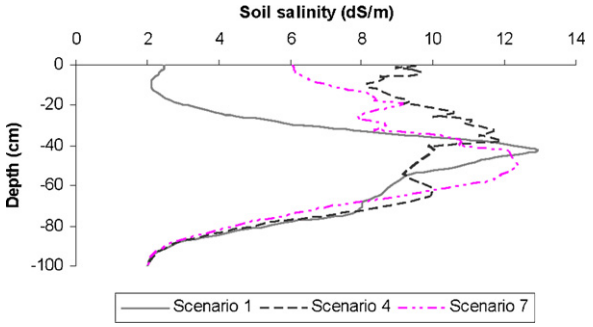

Fig. 9. Soil salinity distribution along vertical section across the plane of symmetry of flow domain (IPED = 20, 30, and 40 cm for scenarios 1, 4, and 7, respectively).

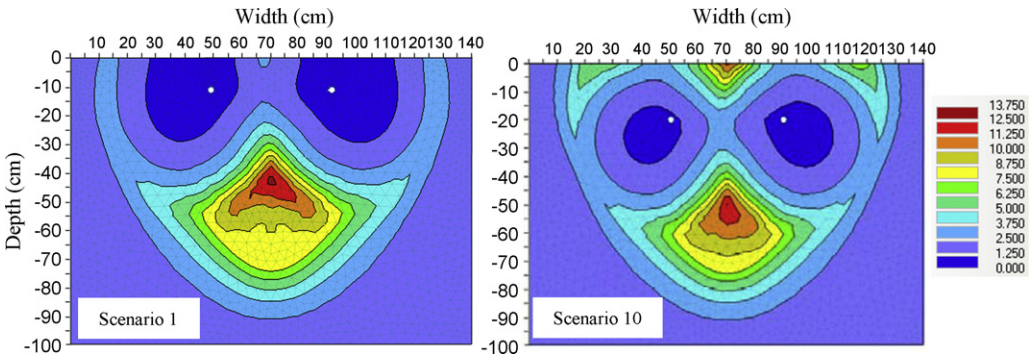

Fig. 10. Spatial distribution of soil salinity at the end of simulation period for different emitter depth scenarios (emitter depth = 10 and 20 cm for scenarios 1 and 10 respectively; unit: dS m^{-1}; white dot indicates to the emitter location).

Table 4
Water balance components in different simulation scenarios expressed as a percent of total applied water.

Scenario number	Root water uptake (%)	Drainage (%)	Root zone storage (%)
1	119.09	7.57	−26.65
2	110.65	7.72	−18.37
3	100.37	8.45	−8.82
4	109.97	9.26	−19.23
5	103.30	9.51	−12.80
6	94.40	10.42	−4.82
7	99.88	13.25	−13.12
8	94.83	13.61	−8.44
9	88.11	14.60	−2.71
10	121.00	8.13	−29.13
11	111.06	8.36	−19.41
12	99.44	9.45	−8.89
13	109.11	10.22	−19.33
14	101.85	10.51	−12.36
15	93.72	11.83	−5.55
16	98.19	14.88	−13.07
17	93.09	15.34	−8.43
18	86.77	16.55	−3.32

for 40 cm IPED with negligible effect of the emitter depth. In general, emitter depth had a negligible effect on amount of applied water taken up by plants roots in APRSDI system. Water balance calculations also showed that as IPED increased, the amount of water percolated to deeper soil layers increased. This is attributed to the significant amount of irrigation water that was located near the flow domain borders far from the zone of maximum root density for long IPED. This amount was unavailable for extraction by plant roots and moved by gravity to deeper soil layers. On the other hand, the effect of irrigation water salinity on the amount of water seeping below the bottom boundary of the flow domain was less distinct. However, Hanson et al. (2008) observed that the salinity of irrigation water under SDI significantly affected the amount of drainage water. Therefore, short IPED with any level of irrigation water salinity is recommended to decrease groundwater contamination risk. Although the amount of drainage water depended mainly on the emitter depth, small difference in amount of drainage water (0.5%) was observed between the 10 and 20 cm emitter depth scenarios. Therefore, emitter depth appears to have negligible effect on potential groundwater contamination risk for the APRSDI system.

3.5. Effect of soil types on soil water and salinity distribution and root water uptake

To extrapolate our results to other soils, additional simulation scenarios were conducted for sand and sandy loam that is the main soil types in the El-Salam Canal cultivated land. Soil water characteristics were assumed based on previous laboratory measurements conducted by the authors and the initial water content was assumed the same for all soils. The simulation results showed that the difference between the vertical and lateral extension of the wetting front after first irrigation event was limited in loamy sand and sandy loam and the difference was larger in sand as compared to other soils. In addition, it was noted that the vertical component for the wetted zone below the emitter was larger in sand as compared to other soils (results not listed). These results can be attributed to the sand characterized by low water holding capacity as compared to loamy sand and sandy loam. Meanwhile, in sand, the gravity force dominated water flow. However, in fine textured soils, there was less available air filled pore space that decreased the infiltration capacity leading to a significant fraction of the applied water to move laterally. In addition, the capillary force governs the water flow. Our results are concurring with the finding of Cote et al. (2003). They concluded that in sand the wetted depth under subsurface drip irrigation was larger than wetted radius while in silt the wetted depth was approximately equal to the wetted radius with same amount of water stored below and above the emitter.

Root water uptake in sand was less than in other soils. This is attributed to the rapid downward movement of water toward the bottom boundary in sand by gravitational force and the higher salinity levels especially below the plant trunk. Salinity results manifested that soil salinity beneath the plant trunk was higher in sand compared to the other soil types. In addition, higher soil salinity below the plant trunk was observed in sand for the case of long IPED regardless of salinity of irrigation water and emitter depth. Therefore, long IPED is not suitable under APRSDI for sand soil even with non-saline irrigation water.

As expected, the amount of water that percolated through the bottom boundary was higher in sand than for other soils. In sand, the applied irrigation water was fully consumed by plants only in case of short IPED with irrigation water salinity of 0 and 1 dS m^{-1}. Therefore, short IPED is recommended for APRSDI only with non-saline and slightly saline irrigation water (1 dS m^{-1}) in sand regardless of emitter depth.

4. Summary and conclusion

Studying wetting and salinity patterns under different geometric design of APRSDI is an efficient way to reduce water losses, quantify the downward leaching of salts, avoid groundwater contamination risk, and create suitable irrigation schedule. In the present study, the HYDRUS-2D/3D model was used to investigate the impact of IPED, emitter depth, and irrigation water salinity levels under APRSDI for growing tomato on soil moisture dynamics, soil salinity distribution, and water balance components. The

numerical simulation of APRSDI in loamy sand included three inter-plant emitter distances (20, 30, and 40 cm), two emitter depths (10 and 20 cm), and three irrigation water salinity levels (0, 1, and 2 dS m^{-1}) with a 40-day simulation period. The simulation results showed that higher moisture content was observed near the domain borders by the end of simulation period in case of long IPED and below the plant trunk in case of short IPED. Therefore, short IPED is appropriate to sustain a considerable amount of soil moisture in the zone of maximum root density. The emitter depth showed an obvious impact on the vertical extension of the wetting front above and beneath the emitter. Deeper wetting front occurred in case of deep emitter depth while the wetting front reached the soil surface in case of shallow emitter depth only. Nevertheless, the fluctuations in soil moisture content at top soil layer were more pronounced in case of shallow emitter depth.

The salinity of irrigation water played a major role in the shape of the soil salinity pattern. Considerable leaching occurred in the top 30 cm soil layer for non-saline irrigation water with higher salinity levels between the 40 and 65 cm soil depths directly below the plant trunk. However, higher salinity levels were observed at soil surface at location of plant and between the 50 and 70 cm depth for the 1 and 2 dS m^{-1} scenarios. Therefore, APRSDI is more suitable with non-saline irrigation water, especially for shallow rooted plants. Simulation also revealed that as the IPED and emitter depth increased, soil salinity at the top soil layer increased while soil salinity in the deeper layers was approximately the same. Therefore, short IPED and shallow emitter are preferable especially with shallow rooted plants. The root water uptake rate depended mainly on soil moisture content and soil salinity levels in the root zone. As salinity of irrigation water increased, root water uptake decreased. The effect of irrigation water salinity was more pronounced for long IPED. Therefore, long IPED is inappropriate when using brackish irrigation water. Regardless of irrigation water salinity, root water uptake rate was also influenced by the geometric design of APRSDI. As IPED increased, root water uptake rate decreased while the emitter depth did not show any significant effect on root water uptake rate. Therefore, short IPED is suitable in APRSDI especially for plant with limited lateral root extension. Water balance calculation showed that the effect of irrigation water salinity and emitter depth on the amount of applied water extracted by plant roots was negligible in case of short IPED while irrigation water salinity had a considerable effect on root water uptake in case of long IPED. On the other hand, as IPED increased, the amount of water that percolated below the bottom boundary of the flow domain increased. However, the effect of emitter depth and irrigation water salinity was less pronounced. Therefore, short IPED with any level of irrigation water salinity is recommended to minimize groundwater contamination risk.

Comparison between soil types revealed that APRSDI is not suitable for sandy soils and long IPED even if non-saline irrigation water is used. However, sandy loam followed the same trend as loamy sand.

Overall, for loamy sand, APRSDI with non-saline irrigation water was more efficient with short IPED especially with plant of limited root extension. Moreover, long IPED is inappropriate when using brackish irrigation water. Both deep and shallow emitter depths can be used in APRSDI considering more care for periodic leaching in case of deep emitter depth to remove excess salt accumulated close to the soil surface when using saline irrigation water.

References

Abou Lila, T.S., Balah, M.I., Hamed, Y.A., 2005. Solute infiltration and spatial salinity distribution behavior for the main soil types at El-Salam Canal project cultivated land. Port Said Eng. Res. J. 9, 242–253.

Ajdary, K., Singh, D.K., Singh, A.K., Khanna, M., 2007. Modelling of nitrogen leaching from experimental onion field under drip fertigation. Agric. Water Manage. 89, 15–28.

Allen, R., Pereira, L., Raes, D., Smith, M., 1998. Crop Evapotranspiration: Guidelines for Computing Crop Water Requirements. Food and Agriculture Organization of the United Nations, Rome.

Beven, K., Henderson, D., Reeves, A., 1993. Dispersion parameters for undisturbed partially saturated soil. J. Hydrol. 143, 19–43.

Celia, M.A., Bouloutas, E.T., Zarba, R.L., 1990. A general mass-conservative numerical solution for the unsaturated flow equation. Water Resour. Res. 26, 1483–1496.

Cote, C.M., Bristow, K.L., Charlesworth, P.B., Cook, F.J., Thorburn, P.J., 2003. Analysis of soil wetting and solute transport in subsurface trickle irrigation. Irrig. Sci. 22, 143–156.

Cote, C.M., Bristow, K.L., Ford, E.J., Verburg, K., Keating, B., 2001. Measurement of water and solute movement in large undisturbed soil cores: analysis of Macknade and Bundaderg data. CSIRO Land and Water. Technical Report 07/2001.

Du, T., Kang, S., Hu, X., Yang, X., 2005. Effect of alternate partial root-zone drip irrigation on yield and water use efficiency of cotton. Sci. Agric. Sin. 38, 2061–2068.

Du, T., Kang, S., Zhang, J., Li, F., Hu, X., 2006. Yield and physiological responses of cotton to partial root-zone irrigation in the oasis field of northwest China. Agric. Water Manage. 84, 41–52.

Feddes, R.A., Kowalik, P.J., Zaradny, H., 1978. Simulation of field water use and crop yield. John Wiley & Sons, New York.

Gardenas, A.I., Hopmans, J.W., Hanson, B.R., Simunek, J., 2005. Two-dimensional modelling of nitrate leaching for various fertigation scenarios under microirrigation. Agric. Water Manage. 74, 219–242.

Gencoglan, C., Altunbey, H., Gencoglan, S., 2006. Response of green beanto subsurface drip irrigation and partial root-zone drying irrigation. Agric. Water Manage. 84, 274–280.

Hafez, A., 2005. Investigation of El-Salam Canal project in northen Sinai, Egypt. Phase I: environmental baseline, soil and water quality studies. In: Ninth International Water Technology Conference, IWTC9 2005, Sharm El-Sheikh, Egypt.

Hanson, B.R., Hopmans, J.W., Simunek, J., 2008. Leaching with subsurface drip irrigation under saline shallow groundwater conditions. Vadose Zone J. 7, 810–818.

Hanson, B., Simunek, J., Hopmans, J.W., 2006. Evaluation of urea–ammonium–nitrate fertigation with drip irrigation using numerical modeling. Agric. Water Manage. 86, 102–113.

Hillel, D., 1998. Environmental Soil Physics. Academic Press, Inc., 525 B Street, Suit 1900, San Diego, CA 92101-4495.

Huang, Z., Qi, X., Fan, X., Hu, C., Zhu, D., Li, P., Qiao, D., 2010. Effects of alternate partial root-zone subsurface drip irrigation on potato yield and water use efficiency. Ying Yong Sheng Tai Xue Bao 21, 79–83.

Kang, S., Zhang, J., 2004. Controlled alternate partial root-zone irrigation: its physiological consequences and impact on water use efficiency. J. Exp. Bot. 55, 2437–2446.

Kidra, C., Cetin, M., Dasgan, H., Topcu, S., Kaman, H., Ekici, B., Derici, M., Ozguven, A., 2004. Yield response of greenhouse grown tomato to partial root drying and conventional deficit irrigation. Agric. Water Manage. 69, 191–201.

Lazarovitch, N., Simunek, J., Shani, U., 2005. System-dependent boundary condition for water flow from subsurface source. Soil Sci. Soc. Am. J. 69 (1), 46–50.

Maas, E.V., 1990. Crop salt tolerance. In: Tanji, K.K. (Ed.), Agricultural Salinity Assessment and Management. ASCE Manuals and Report on Engineering Practice 71. American Society of Civil Engineers, New York, pp. 262–304.

Phogat, V., Yadav, A.K., Malik, R.S., Kumar, S., Cox, J., 2010. Simulation of salt and water movement and estimation of water productivity of rice crop irrigated with saline water. Paddy Water Environ. 8, 333–346.

Rashed, A., Khalifa, E., Fahmy, H., 2003. Paddy rice cultivation in irrigated water managed saline sodic lands under reclamation, Egypt. In: The 9th ICID International Drainage Workshop, Utrecht, Netherlands.

Richards, L.A., 1931. Capillary conduction of liquid in porous media. Physics 1, 318–333.

Saeed, H., Grove, I., Kettlewell, P., Hall, P., 2008. Potential of partial root zone drying as an alternative irrigation technique for potatoes. Ann. Appl. Bot. 152, 71–80.

Selim, T., Berndtsson, R., Persson, M., Somaida, M., El-Kiki, M., Hamed, Y., Mirdan, A., 2011. Evaluation of subsurface trickle irrigation with brackish water. Unpublished results.

Sepaskhah, A., Ahmadi, S., 2010. A review on partial root-zone drying irrigation. Int. J. Plant Prod. 4, 241–258.

Shani-Dashtgol, A., Jaafari, S., Abbasi, N., Malaki, A., 2006. Effects of alternate furrow irrigation (PRD) on yield quantity and quality of sugarcane in southern farm in Ahvaz. In: Proceedings of the National Conference on Irrigation and Drainage Networks Management, Shahid Chamran University of Ahvaz, pp. 565–572.

Simunek, J., Hopmans, J.W., 2009. Modelling compensated root water and nutrient uptake. Ecol. Model. 220, 505–521.

Simunek, J., van Genuchten, M.Th., Sejna, M., 2008. Development and applications of the HYDRUS and STANMOD software package and related codes. Vadose Zone J. 7 (2), 587–600.

Skaggs, T.H., Trout, T.J., Simunek, J., Shouse, P.J., 2004. Comparison of HYDRUS-2D simulations of drip irrigation with experimental observations. J. Irrig. Drain. Eng. 130 (4), 304–310.

Stoll, M., Loveys, B., Dry, P., 2000. Hormonal changes induced by partial root-zone drying of irrigated grapevine. J. Exp. Bot. 51, 1627–1634.

Wang, J., Kang, S., Li, F., Zhang, F., Li, Z., Zhang, J., 2008. Effects of alternate partial root-zone irrigation on soil microorganism and maize growth. Plant Soil 302, 45–52.
Zhou, Q., Kang, S., Zhang, L., Li, F., 2007. Comparison of APRI and HYDRUS-2D models to simulate soil water dynamics in a vineyard under alternate partial root-zone drip irrigation. Plant Soil 291, 211–223.
Zhou, Q., Kang, S., Li, F., Zhang, L., 2008. Comparison of dynamic and static APRI-models to simulate soil water dynamics in a vineyard over the growing season under alternate partial root-zone drip irrigation. Agric. Water Manage. 95, 767–775.

Tarek Selim[a,b,*]
[a] *Civil Engineering Department, Faculty of Engineering, Port Said University, Egypt*
[b] *Department of Water Resources Engineering, Lund University, Box 118, 221 00 Lund, Sweden*

Ronny Berndtsson[a,b]
[a] *Department of Water Resources Engineering, Lund University, Box 118, 221 00 Lund, Sweden*
[b] *Center for Middle Eastern Studies, Lund University, Box 201, 221 00 Lund, Sweden*

Magnus Persson
Department of Water Resources Engineering, Lund University, Box 118, 221 00 Lund, Sweden

Mohamed Somaida
Mohamed El-Kiki
Yasser Hamed
Ahmed Mirdan
Civil Engineering Department, Faculty of Engineering, Port Said University, Egypt

Qingyun Zhou
Hydraulic Engineering Department, Tianjin Agricultural University, Tianjin 300384, China

[*] Corresponding author at: Civil Engineering Department, Faculty of Engineering, Port Said University, Egypt.
E-mail address: eng_tarek_selim@yahoo.com (T. Selim)

29 July 2011

21 November 2011

23 November 2011
Available online 15 December 2011